BMC Medical Imaging

RESEARCH

Open Access

Atypical ductal hyperplasia diagnosed by US-guided core needle biopsy: clinical, pathological and US features associated with upgrading to malignancy

Jun Kang Li[1,2†], Yong Jie Xu[3†], Rui Lan Niu[1], Nai Qin Fu[1], Zhi Ying Jin[1], Shi Yu Li[1], Yu Chen Liu[4,5*†] and Zhi Li Wang[1,5*†]

Abstract

Background To develop a predictive model to identify atypical ductal hyperplasia (ADH) that was underestimated by US-guided core needle biopsy (CNB) and to evaluate the risk factors for underestimation for ADH with intraductal papilloma diagnosed by CNB.

Methods In this retrospective study, 300 CNB-diagnosed ADH lesions in 291 consecutive women between January 2014 and July 2023 were included and divided into training set ($n=181$), internal validation set ($n=54$), and external validation set ($n=65$). The review included clinical, pathological, and US features, as well as final outcomes. Multivariate logistic regression was employed to establish predictive model and to evaluate risk factors. Model performance was evaluated using area under the receiver operating characteristic curve (AUC), calibration curve, decision curve analysis, and utility (patient stratification into low and high-risk groups). Model was validated both internally and externally by calculating its performance on validation sets.

Results The upgrade rate to malignancy was 51.0%. Predictors included in the model were age, the pathological pattern of ADH with intraductal papilloma or ADH alone, Ki-67 positivity, and imaging-pathological discordance. The AUC was 0.915 (95% CI: 0.858, 0.955) in the training set, 0.906 (95% CI: 0.785, 0.972) in the internal validation set, and 0.934 (95% CI: 0.836, 0.983) in the external validation set. Using a cutoff value of 0.11, 38.3% of nonmalignant lesions in the training set were stratified into low-risk group with an upgrade rate of 4.1%. Similar results were obtained in the validation sets. For ADH with intraductal papilloma, age and imaging-pathological discordance were the independent risk factors for malignancy upgrading.

†Jun Kang Li and Yong Jie Xu are the co-first authors that have equal contributions.

Zhi Li Wang and Yu Chen Liu are the co-corresponding authors that have equal contributions.

*Correspondence:
Yu Chen Liu
sisi5203020@163.com
Zhi Li Wang
wzllg@sina.com

Full list of author information is available at the end of the article

Conclusions The model established to predict ADH upgrading can help in individualized risk management. If predictors of non-upgraded ADH lesions can be confirmed with larger studies, more than one-third of non-malignant lesions are expected to be candidates for non-excision.

Trial registration This is a retrospective study.

Keywords Atypical ductal hyperplasia, Ultrasound, Breast neoplasms, Biopsy

Background

Atypical ductal hyperplasia (ADH) is an intraductal proliferation that has cytological and architectural features similar to low-grade ductal carcinoma in situ (DCIS) but does not meet the diagnostic criteria for low-grade DCIS [1]. The distinction between ADH and DCIS is primarily based on a quantitative criterion with a threshold of 2 mm in maximum dimension or a threshold of 2 ductal spaces involved. In recent years, detection of ADH on core needle biopsy (CNB) has increased due to the increase rates of breast cancer screening [2]. The prevalence of ADH ranged from 3 to 4% in all types of image-guided CNB and ranged from 0.9 to 2.7% in US-guided CNB [3]. The potential for upgrading to malignancy in the final results due to the sampling limitations of CNB, with upgrade rates ranging from 0 to 84% in previous studies [4, 5]. Therefore, current clinical practice has recommended that ADH cases diagnosed by CNB undergo surgical resection [6, 7]. Although proactive management of ADH can help prevent such lesions from progressing to malignancy, it carries the risk of overdiagnosis and overtreatment. The upgrade rate for the ADH cases diagnosed by percutaneous biopsy and managed with surveillance was 5%, which was significantly lower than that for surgically excised cases [8]. Active surveillance, chemoprevention, and risk reduction strategies are also management options for patients with ADH [2, 3, 9]. Therefore, the identification of ADH cases underestimated by CNB will be of great importance in selecting the most appropriate management strategy.

Risk factors that differentiate ADH upgrade from non-upgrade have not been definitively identified, although factors such as clinical data (age, family history, mass palpation, associated symptom), imaging findings (calcifications on US or mammography, BI-RADS category), biopsy technique, imaging guidance (mammography, US, MRI), histological variables, and biopsy device (CNB, vacuum-assisted biopsy) have been previously evaluated [10–12]. The role of estrogen receptor (ER), progesterone receptor (PR), human epidermal growth factor receptor 2 (HER2), and Ki-67 expression in predicting ADH lesions diagnosed by CNB that are likely to upgrade to malignant at surgery has not been reported. In addition, a significant proportion of Asian women have dense breasts, and some choose to undergo breast cancer screening with ultrasound alone, rather than mammography, due to the reduced sensitivity of the latter in individuals with dense breasts. Directly applying the results of previous studies involving mammography to patients who have undergone ultrasonography alone may not yield satisfactory results. Besides, ADH may be co-diagnosed with additional pathological findings such as fibroadenoma, adenosis, and intraductal papilloma. CNB-diagnosed intraductal papilloma may also be surgically upgraded to malignancy and have diverse postoperative histopathological findings [13]. The upgrade rate and risk factors for lesions of ADH with intraductal papilloma are unclear.

Thus, the purpose of this study was to develop a predictive model to identify ADH lesions that were underestimated by US-guided CNB and to evaluate the risk factors for underestimation of ADH with intraductal papilloma diagnosed by CNB.

Methods

Study population

All procedures were performed in compliance with relevant laws and institutional guidelines and have been approved by the institutional review board. Informed consent was waived due to the retrospective design. Of 14,433 consecutive women who underwent breast US examination and US-guided CNB at the First Medical Center of the PLA General Hospital (institution 1) and the Ninth Medical Center of the PLA General Hospital (institution 2) between January 2014 and July 2023, 340 women were pathologically diagnosed with ADH by CNB and were initially considered for inclusion in this study. In the case of multiple lesions in the ipsilateral breast, only the most suspicious one was included. Of the 340 patients, 49 were excluded according to the following exclusion criteria: patients underwent breast-conserving surgery in the ipsilateral breast ($n = 1$); confirmed with lymph node metastasis preoperatively ($n = 4$); concomitant malignant lesion in the ipsilateral or contralateral breast ($n = 11$); did not undergo open excision or were lost to follow-up ($n = 33$). Therefore, 291 women with 300 criteria-matched lesions were included in this study. All patients subsequently underwent surgery.

US examination and US-guided CNB procedures

All patients underwent breast US examination before US-guided CNB. Both US examination and CNB were performed by one of the two radiologists (L.J.K. and

W.Z.L., with more than 10 years of experience in breast US and US-guided CNB). A MyLab Twice US system (Esaote) with an LA523 transducer at 4–13 MHz or an iU22 US system (Philips Healthcare) with an L12-5 transducer at 5–12 MHz were used.

US-guided CNB was performed with a 14-, 16- or 18-gauge core biopsy needle (Bard Peripheral Vascular, Inc.) using a freehand technique. Penetration depths were set at 22 mm. The biopsy procedure was repeated 2–6 times for different areas of the target lesion. The lesion size (maximum diameter measured by US), distance from the nipple, needle gauge, and number of cores were recorded.

Histopathological analysis

Histopathological results of CNB and surgical resected specimens were evaluated based on the diagnostic criteria of the WHO guidelines [1]. The data of pathological pattern (ADH alone or co-diagnosed with fibroadenoma, adenosis, and intraductal papilloma), negative edge of the core, the max extent of ADH foci, the number of ADH foci, and molecular testing (ER, PR, HER2, and Ki-67) were recorded. The cut-off for ER and PR positivity was 10% of nuclei stained. Lesions with erbB-2 receptor staining 3 + or 2 + with fluorescence in situ hybridization positivity were defined as HER2 positive. The cut-off for Ki-67 positivity was 14% [14].

Image analysis

Image analysis and clinical information collection were performed by two radiologists (X.Y.J. and J.Z.Y., with more than 5 years of experience in breast US) who were blinded to the surgical pathology results. Disagreements were adjudicated and resolved by a third radiologist (W.Z.L.). Clinical data including age, presence of nipple discharge, and palpability of the lesion were collected from the medical records. The lesion types were divided into mass-like lesions and non-mass-like lesions according to previous literature [15]. The following US features were described according to the American College of Radiology Breast Imaging-Reporting and Data System (BI-RADS) [16]: shape, margin, orientation, posterior features, calcifications, and vascularity. The composition was divided into solid and complex cystic and solid.

Statistical analysis

Patients who underwent CNB at institution 1 from January 2014 to July 2021 were divided into the training set, patients who underwent CNB at institution 1 from August 2021 to July 2023 were divided into the internal validation set, and all patients who underwent CNB at institution 2 were divided into the external validation set. The upgrade was defined as when a lesion initially diagnosed as ADH via core needle biopsy but diagnosed as malignant at surgery. The imaging-pathology correlation was assessed based on whether the pathology results could reasonably explain the imaging findings. For ADH lesions diagnosed by CNB, the imaging and pathology results were considered to be concordant if the BI-RADS category was 3–4 A, and discordant if the BI-RADS category was 4B, 4 C, or 5.

Statistical comparisons were performed by using the Mann-Whitney U test for continuous variables and the $\chi 2$ test or Fisher's exact test for categorical variables. Univariate binary logistic regression analysis was performed on the training set to analyze the correlations between clinical data, biopsy pathological findings, and US features and to upgrade to malignancy. When zeros caused problems in the computation of the odds ratio or its standard error, 0.5 was added to all cells [17]. Multivariate binary logistic regression analysis was performed using variables selected according to the results of univariate analysis ($P < .05$). For multiple comparisons, a string P value < 0.001 was used to determine the statistical significance of the result. The variance inflation factor was evaluated among the covariates, and a variance inflation factor of more than 5.0 was interpreted as indicating multicollinearity. The proportion of missing values for ER, PR, HER2, and Ki-67 was 4.3%, 4.3%, 35.6%, and 16.7%, respectively. Therefore, the HER2 was removed from the study. Using all baseline characteristics and final outcomes, multiple imputation was used for the missing values of ER, PR, and Ki-67 to generate 20 imputed data sets, providing pooled adjusted odds ratios (ORs) with 95% CIs [18]. The discriminative ability of the model was assessed using the area under the receiver operating characteristic curve (AUC) and further validated by the validation sets. For the training set, the AUC was calculated as the median value of the 20 imputed datasets, while the ROC was obtained from the complete case analysis. The consistency between the observed probability and the predicted probability was evaluated by the calibration curve using the Hosmer-Lemeshow goodness-of-fit test. For the validation sets, both ROC and calibration plots were obtained from the complete case analysis. Decision curve analysis was used to assess the clinical benefit of the model. The cutoff values obtained in the training set were used to stratify lesions in the validation sets into low-risk or high-risk groups. The utility of the model was evaluated by sensitivity, specificity, and upgrade rate of low-risk or high-risk groups based on the cutoff value in the training set. Youden's index was used to determine the optimal cutoff value. According to the Third International Consensus Conference on lesions of uncertain malignant potential in the breast (B3 lesions), patients scheduled for radiological surveillance need to meet an underestimation rate of less than 5% for invasive cancer and less than 10% for DCIS [7]. Therefore,

in order to align with the clinical environment, the cutoff points of upgrade rate less than 5% and less than 10% were determined in the training set, with the objective of identifying candidates for non-excision. The performance of all cutoff points was validated in both the internal and external validation sets.

Univariate and multivariate analysis was also been used to evaluate the risk factors for CNB-diagnosed ADH with intraductal papilloma that to be upgraded to malignancy at surgery. The missing values of ER, PR, and Ki-67 were treated as positive, negative, and unknown. Statistical analyses were performed using SPSS 25.0 (SPSS Inc) and R 4.0.5 (The R Project for Statistical Computing). Differences were considered statistically significant at two-sided *P* values less than 0.05.

Results

Patient characteristics

The median age of the 291 women with 300 lesions was 47 years (interquartile range [IQR], 41–58 years; range, 18–87 years). Histopathological examination of surgical resection specimens revealed 153 malignant and 147 non-malignant lesions. Thus, the upgrade rate of ADH lesions at CNB was 51.0% (153 of 300). Of the 300 lesions, 181 (60.3%) were classified in the training set, 54 (18.0%) in the internal validation set, and 65 (21.7%) in the external validation set (Fig. 1). The median size of all lesions was 1.3 cm (IQR, 0.9–1.9 cm; range, 0.4–8.0 cm). Baseline characteristics in training and validation sets are summarized and compared in Table 1. Upgrade rates were similar between the training and validation sets. The most common malignant lesions were DCIS and invasive ductal carcinoma (Table 2). No adverse events were reported during US examinations and US-guided CNB.

Establishment of predictive model for the upgrade of ADH

The univariate and multivariable regression analysis of clinical, biopsy pathological findings, and US features in the training set is shown in Table 3. According to the results of the univariate analysis, the features of age, lesion size, pathological pattern, ER status, PR status, Ki-67 status, lesion types, shape, margin, calcifications on ultrasound, vascularity, imaging-pathology correlation (Figs. 2 and 3) were included in the multivariate binary logistic regression analysis to establish a predictive model. The multiple imputed datasets were used and ORs with 95% CIs were provided. Features of age (OR, 1.09; 95 CI%: 1.05, 1.14; $P<.001$), pathological pattern of ADH with intraductal papilloma (OR, 30.26; 95% CI: 1.86, 491.69; $P=.02$) or ADH alone (OR, 36.21; 95% CI: 2.24, 586.98; $P=.01$), Ki-67 positivity (OR, 5.52; 95% CI: 1.29, 23.54; $P=.02$), and imaging-pathological discordance (OR, 7.08; 95% CI: 2.28, 22.06; $P<.001$) remained independent predictive factors for upgrade of ADH (Table 3). Equation for the predictive model were detailed in Table A.1. The AUC was 0.912 (range, 0.903–0.922) for multiple imputed data sets, 0.915 (95% CI: 0.858, 0.955) for complete case analysis in the training set, 0.906 (95% CI: 0.785, 0.972) in the internal validation set, and 0.934 (95% CI: 0.836, 0.983) in the external validation set (Fig.

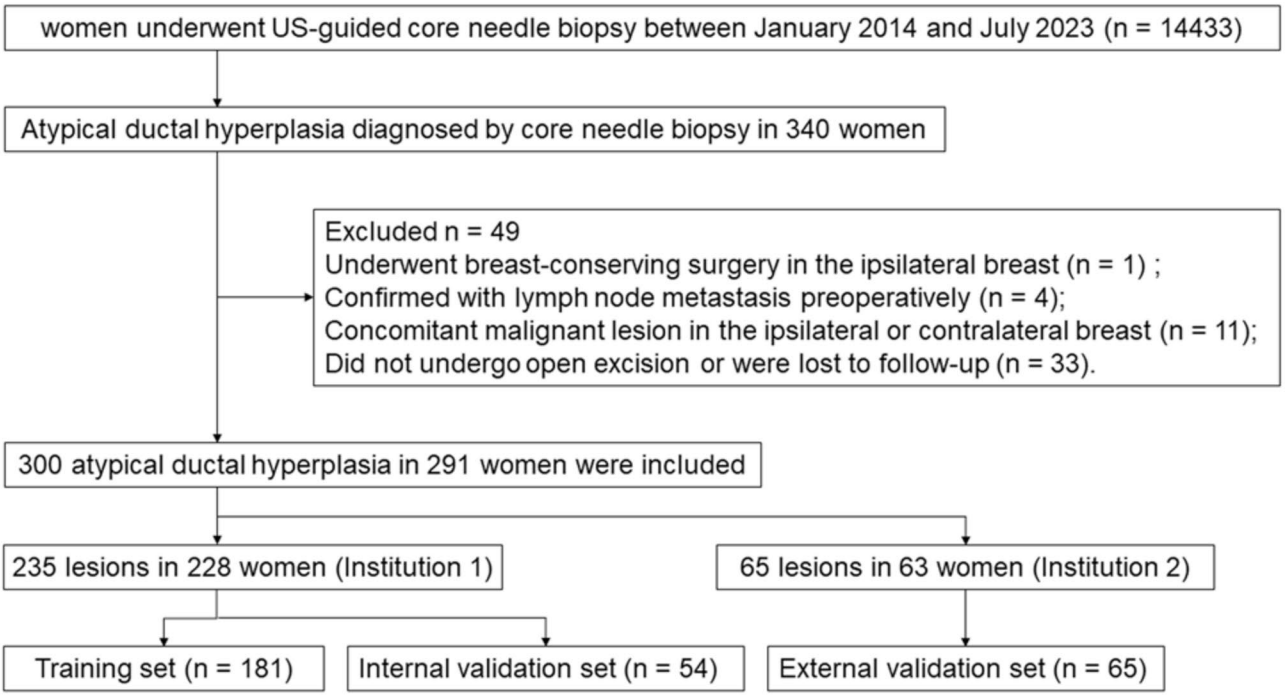

Fig. 1 Flowchart of the process of patient enrollment

Table 1 Baseline characteristics in training and validation sets

Variable	Training set	Internal validation set	*P* Value	External validation set	*P* Value
Number of lesions	181	54		65	
Median age (year)	47(41–55)[a]	48(40–61)[a]	0.55	47(41–63)[a]	0.38
Median size (cm)	1.3(0.9–2.1)[a]	1.1(0.9–1.8)[a]	0.27	1.4(0.9–1.4)[a]	0.97
Nipple discharge			0.35		0.73
Absent	144(79.6)	46(85.2)		53(81.5)	
Present	37(20.4)	8(14.8)		12(18.5)	
Palpability			0.17		0.29
Impalpable	54(29.8)	11(20.4)		24(36.9)	
Palpable	127(70.2)	43(79.6)		41(63.1)	
Biopsy needle			< 0.001		0.001
14-Gauge	0	0		43(66.2)	
16-Gauge	105(58.0)	13(24.1)		22(33.8)	
18-Gauge	76(42.0)	41(75.9)		0	
Number of cores			0.01		0.98
2	58(32.0)	6(11.1)		20(30.8)	
3	107(59.2)	42(77.8)		39(60.0)	
4–6	16(8.8)	6(11.1)		6(9.2)	
Distance from nipple			0.57		0.31
≤ 2 cm	105(58.0)	29(53.7)		33(50.8)	
> 2 cm	76(42.0)	25(46.3)		32(49.2)	
Pathological pattern			0.22		0.40
With fibroadenoma	12(6.6)	2(3.7)		7(10.8)	
With adenosis	46(25.4)	8(14.8)		12(18.4)	
With intraductal papilloma	60(33.0)	18(33.3)		26(40.0)	
ADH alone	63(34.8)	26(48.2)		20(30.8)	
ER status($n = 287$)			0.34		0.33
Negative	22(12.6)	4(7.8)		5(8.1)	
Positive	152(87.4)	47(92.2)		57(91.9)	
PR status($n = 287$)			0.97		0.25
Negative	27(15.5)	8(15.7)		6(9.7)	
Positive	147(84.5)	43(84.3)		56(90.3)	
Ki-67 status($n = 250$)			0.95		0.44
Negative	105(71.9)	34(72.3)		44(77.2)	
Positive	41(28.1)	13(27.7)		13(22.8)	
Negative edge of core			0.69		0.60
Yes	86(47.5)	24(44.4)		28(43.8)	
No	95(52.5)	30(55.6)		36(56.2)	
Max extent of ADH foci			0.38		0.74
≤ 0.1 cm	75(41.4)	26(48.1)		28(43.8)	
> 0.1 cm	106(58.6)	28(51.9)		36(56.2)	
ADH foci number			0.006		0.18
≤ 2	57(31.5)	28(51.9)		26(40.6)	
>2	124(68.5)	26(48.1)		38(59.4)	
Lesion types			0.59		0.80
Mass-like lesion	145(80.1)	45(83.3)		53(81.5)	
Non-mass-like lesion	36(19.9)	9(16.7)		12(18.5)	
Shape			0.60		0.76
Round/Oval	25(13.8)	9(16.7)		8(12.3)	
Irregular	156(86.2)	45(83.3)		57(87.7)	
Margin			0.42		0.41
Circumscribed	63(34.8)	22(40.7)		19(29.2)	
Not circumscribed	118(65.2)	32(59.3)		46(70.8)	
Composition			0.89		0.46

Table 1 (continued)

Variable	Training set	Internal validation set	*P* Value	External validation set	*P* Value
Solid	175(96.7)	52(96.3)		64(98.5)	
Complex cystic and solid	6(3.3)	2(3.7)		1(1.5)	
Orientation			0.01		0.22
Parallel	161(89.0)	41(75.9)		54(83.1)	
Not parallel	20(11.0)	13(24.1)		11(16.9)	
Posterior features			0.54		0.57
No posterior features	177(97.8)	52(96.3)		65(100)	
Shadowing /Enhancement	4(2.2)	2(3.7)		0	
Calcifications on ultrasound			0.07		0.65
Absent	136(75.1)	34(63.0)		47(72.3)	
Present	45(24.9)	20(37.0)		18(27.7)	
Duct changes			0.09		0.81
Absent	166(91.7)	53(98.1)		59(90.8)	
Present	15(8.3)	1(1.9)		6(9.2)	
Vascularity			0.14		0.79
Absent	94(51.9)	22(40.7)		35(53.8)	
Present	87(48.1)	32(59.3)		30(46.2)	
Imaging-pathology correlation			0.38		0.74
Concordant	96(53.0)	25(46.3)		36(55.4)	
Discordant	85(47.0)	29(53.7)		29(44.6)	

Note: Unless otherwise specified, variables are expressed as numbers of lesions with percentages in parentheses. ER = estrogen receptor, PR = progesterone receptor, ADH = atypical ductal hyperplasia

[a] Variables are expressed as medians with interquartile ranges in parentheses

Table 2 Histopathology results of core needle biopsy and surgery

Surgical histopathology results	CNB histopathology results			
	With fibroadenoma(*n* = 21)	With adenosis(*n* = 66)	With intraductal papilloma(*n* = 104)	ADH alone (*n* = 109)
Malignant				
Ductal carcinoma in situ	1	15	38	50
Invasive ductal carcinoma	0	6	5	23
Papillary ductal carcinoma in situ	0	0	6	0
Intraductal papillary adenocarcinoma with invasion	0	0	3	0
Encapsulated papillary carcinoma	0	0	1	0
Mucinous adenocarcinoma	0	1	3	1
ADH with or without papilloma	3	24	29	18
Other benign diagnosis	17	20	19	17

Note: ADH = atypical ductal hyperplasia, CNB = core needle biopsy

4). Calibration plots showed that the predicted probabilities of the model were close to the observed probabilities in the training set, while deviated slightly in the validation sets (Fig. 5). The decision curve analysis showed a positive net benefit when the threshold probability was between 0 and 0.7 (Fig. 6).

With the optimal cutoff value of 0.63, the sensitivity of the training set, the internal validation set, and the external validation set were 81.4%, 77.8%, 73.1%, respectively, and the specificity were 86.7%, 90.0%, 90.3%, respectively. Lesions in the training and validation sets were stratified into low-risk and high-risk groups using the cutoff value obtained from the developed model. Using a cutoff value of 0.18, 56.7% of nonmalignant lesions in the training set were stratified into low-risk group with an upgrade rate of 10.5%. Management decision correctly changed from open excision to non-open excision for 34 lesions and incorrectly changed from open excision to non-open excision for 4 lesions. Using a cutoff value of 0.11, 38.3% of nonmalignant lesions in the training set were stratified into low-risk group with an upgrade rate of 4.1%. Management decision correctly changed from open excision to non-open excision for 23 lesions, and incorrectly changed from open excision to non-open excision for only one lesion. Similar results were obtained in the internal and external validation sets (Table 4). The

Table 3 Univariate and multivariable logistic regression analysis of the clinical data, biopsy pathological findings, and US features to predict upgrading of atypical ductal hyperplasia in the training set

Variable	Univariable Analysis		Multivariable Analysis	
	Odds Ratio	***P* Value**	**Odds Ratio**	***P* Value**
Median age (year)	1.07(1.04,1.10)	< 0.001	1.09(1.05,1.14)	< 0.001
Median size (cm)	2.24(1.55,3.24)	< 0.001	1.42(0.77,2.64)	0.26
Nipple discharge				
Absent	1 (reference)			
Present	0.92(0.45,1.89)	0.82		
Palpability				
Impalpable	1 (reference)			
Palpable	1.47(0.78,2.79)	0.24		
Biopsy needle				
16-Gauge	1 (reference)			
18-Gauge	1.40(0.77,2.54)	0.27		
Number of cores		0.49		
2	1 (reference)			
3	1.47(0.77.2.79)	0.24		
4–6	1.48(0.48,4.50)	0.49		
Distance from nipple				
≤ 2 cm	1 (reference)			
> 2 cm	0.97(0.54,1.76)	0.93		
Pathological pattern		< 0.001		
With fibroadenoma	1 (reference)		1 (reference)	
With adenosis	5.32(0.63,45.15)	0.13	7.52(0.46,122.52)	0.15
With intraductal papilloma	15.40(1.87,127.08)	0.01	30.26(1.86,491.69)	0.02
ADH alone	27.50(3.31,228.84)	0.002	36.21(2.24,586.98)	0.01
ER status($n = 225$)				
Negative	1 (reference)		1 (reference)	
Positive	0.15(0.04,0.51)	0.003	1.67(0.03,101.29)	0.81
PR status($n = 225$)				
Negative	1 (reference)		1 (reference)	
Positive	0.15(0.05,0.47)	0.001	0.29(0.01,12.71)	0.52
Ki-67 status($n = 193$)				
Negative	1 (reference)		1 (reference)	
Positive	10.57(3.52,31.78)	< 0.001	5.52(1.29,23.54)	0.02
Negative edge of core				
Yes	1 (reference)			
No	1.51(0.84,2.72)	0.17		
Max extent of ADH foci				
≤ 0.1 cm	1 (reference)			
> 0.1 cm	1.29(0.71,2.33)	0.40		
ADH foci number				
≤ 2	1 (reference)			
>2	1.14(0.61,2.13)	0.69		
Lesion types				
Mass-like lesion	1 (reference)		1 (reference)	
Non-mass-like lesion	4.03(1.79,9.08)	0.001	2.38(0.55,10.35)	0.25
Shape				
Round/Oval	1 (reference)		1 (reference)	
Irregular	3.42(1.35,8.65)	0.01	1.20(0.25,5.74)	0.82
Margin				
Circumscribed	1 (reference)		1 (reference)	
Not circumscribed	3.89(2.03,7.46)	< 0.001	1.24(0.40,3.89)	0.71
Composition				

Table 3 (continued)

Variable	Univariable Analysis		Multivariable Analysis	
	Odds Ratio	*P* Value	Odds Ratio	*P* Value
Solid	1 (reference)			
Complex cystic and solid	4.62(0.53,40.32)	0.17		
Orientation				
Parallel	1 (reference)			
Not parallel	0.87(0.34,2.21)	0.77		
Posterior features				
No posterior features	1 (reference)			
Shadowing /Enhancement	2.71(0.28,26.55)	0.39		
Calcifications on ultrasound				
Absent	1 (reference)		1 (reference)	
Present	3.69(1.73,7.88)	0.001	1.45(0.37,5.64)	0.59
Duct changes				
Absent	1 (reference)			
Present	1.01(0.35,2.92)	0.98		
Vascularity				
Absent	1 (reference)		1 (reference)	
Present	2.68(1.47,4.90)	0.001	2.01(0.77,5.23)	0.15
Imaging-pathology correlation				
Concordant	1 (reference)		1 (reference)	
Discordant	7.64(3.92,14.91)	< 0.001	7.08(2.28,22.06)	0.001

Note: ER = estrogen receptor, PR = progesterone receptor, ADH = atypical ductal hyperplasia. Data in parentheses are 95% CIs

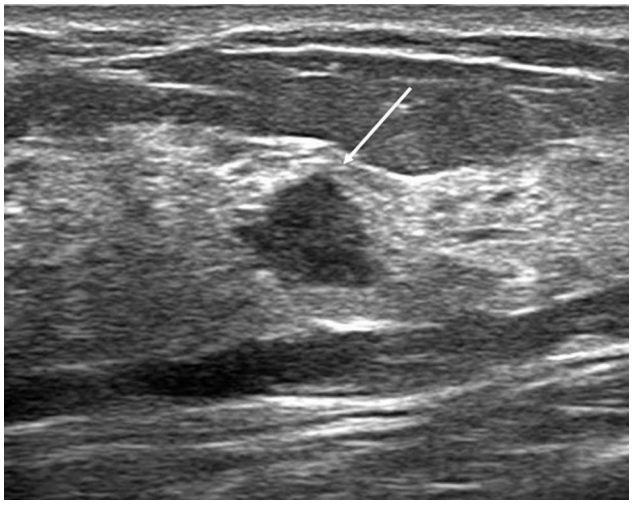

Fig. 2 Image of an unpalpable mass.US shows a hypoechoic solid mass (white arrow) with not circumscribed margin and irregular shape. This lesion was classified as breast imaging reporting and data system category 4A and diagnosed as atypical ductal hyperplasia with adenosis at US-guided core needle biopsy and as adenosis at surgery

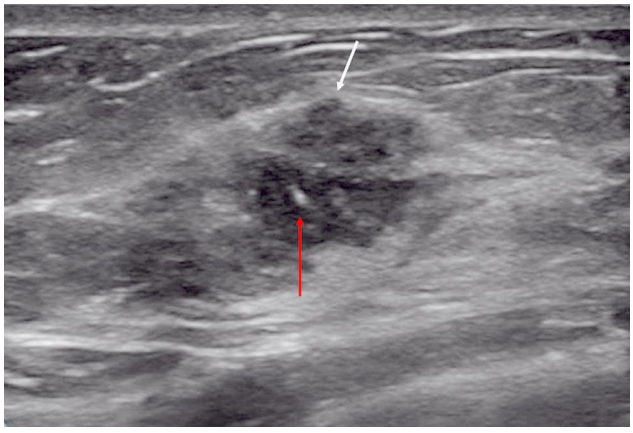

Fig. 3 Image of a palpable mass.US shows a hypoechoic solid mass (white arrow) with not circumscribed margin, irregular shape, and microcalcifications (red arrow). This lesion was classified as breast imaging reporting and data system category 4C and diagnosed as atypical ductal hyperplasia at US-guided core needle biopsy and as ductal carcinoma in situ at surgery

clinical decision-making flowchart based on the prediction model is shown in Fig. 7.

Evaluation of the risk factors for underestimation for ADH with intraductal papilloma and ADH alone

Based on the above findings, the upgrade rate of ADH with intraductal papilloma and ADH alone were significantly higher than that of other types, and additional analysis of risk factors for both types was performed. Among the 104 lesions of ADH with intraductal papilloma, 53.8% (56 of 104) were upgraded to malignancy at surgery. Univariate analysis showed that age (OR, 1.04; 95% CI: 1.01, 1.07; P=.019), lesion size (OR, 2.32; 95% CI: 1.41, 3.82; P=.001), non-mass-like lesion (OR, 3.67; 95% CI: 1.12, 12.04; P=.03), not circumscribed margin (OR, 3.82; 95% CI: 1.68, 8.65; P=.001), presence of calcifications on ultrasound (OR, 5.21; 95% CI: 1.62, 16.74; P=.006), imaging-pathological discordance (OR, 5.07;

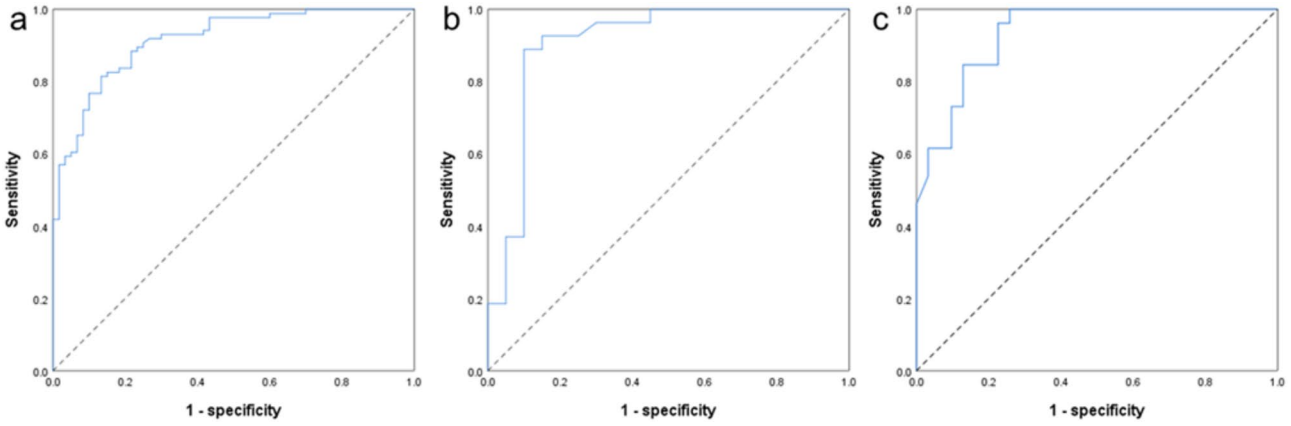

Fig. 4 Receiver operating characteristic curves of the predictive model for atypical ductal hyperplasia underestimated by US-guided core needle biopsy. **a**, in the training set; **b**, in the internal validation set; **c**, in the external validation set

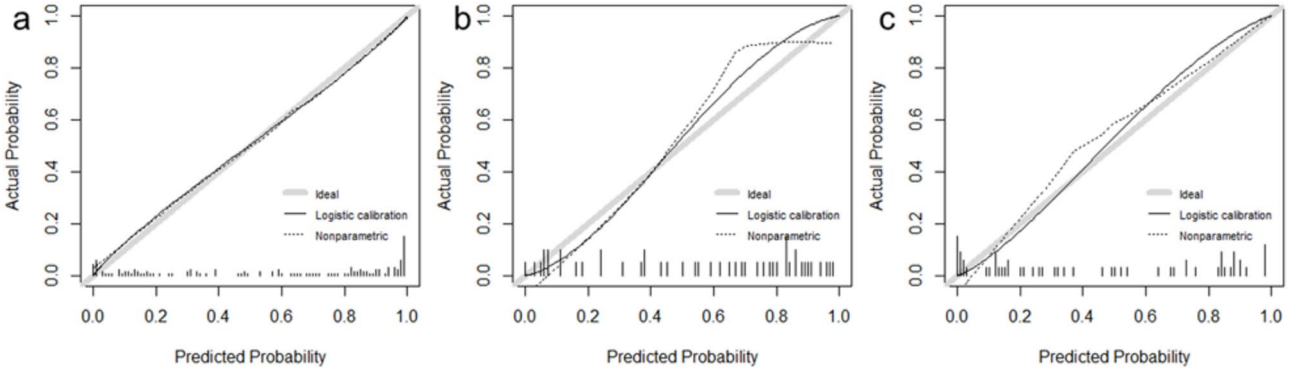

Fig. 5 Calibration curves. The X-axis represents the predicted probability of the model, and the Y-axis represents the actual probability. The diagonal line (Ideal) indicates the reference line in which the predicted probabilities are equal to the actual probabilities, while the solid line represents the performance of the model. **a**, in the training set; **b**, in the internal validation set; **c**, in the external validation set

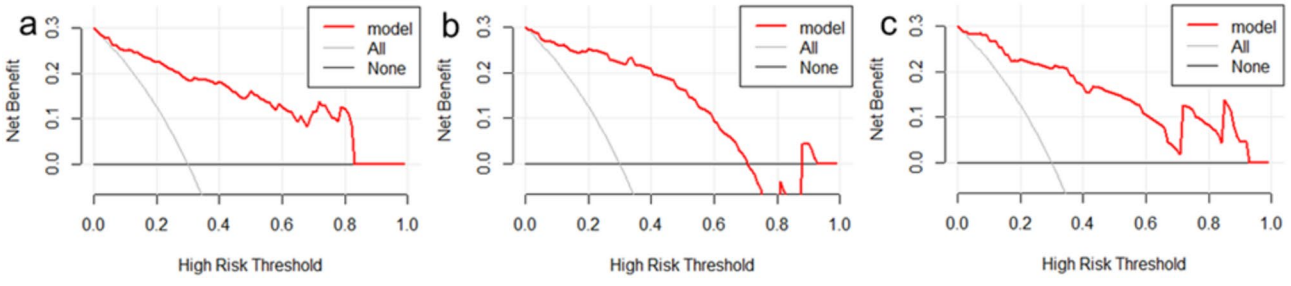

Fig. 6 Decision curve analysis. Tin slash line: assume all patients are upgraded to malignant and undergo surgery; solid horizontal line: assume no patients are upgraded to malignant and do not undergo surgery. **a**, in the training set; **b**, in the internal validation set; **c**, in the external validation set

95% CI: 2.11, 12.15; P<.001), and Ki-67 positivity (OR, 4.50; 95% CI: 1.39, 14.61; P=.012) were positively associated with upgrading (Table A.2). On multivariable analysis, age (OR, 1.06; 95% CI: 1.02, 1.10; P=.005) and imaging-pathological discordance (OR, 3.67; 95% CI: 1.05, 12.83; P=.04) were the independent risk factors for the upgrade of ADH with intraductal papilloma (Table 5).

Among the 109 lesions of ADH with intraductal papilloma, 67.9% (74 of 109) were upgraded to malignancy at surgery. Univariate analysis of the clinical data, biopsy pathological findings, and US features to identify the factors for pure atypical ductal hyperplasia is shown in Table A.3. PR was not included in the multivariate analysis because the variance inflation factor value was more than 5.0. On multivariable analysis, age (OR, 1.18; 95% CI: 1.06, 1.32; P=.002), Ki-67 positivity (OR, 79.76; 95% CI: 3.85, 787.81; P=.005), and imaging-pathological discordance (OR, 18.87; 95% CI: 2.22, 160.37; P=.007) were the independent risk factors for the upgrade of ADH alone (Table 6).

Table 4 Model utility based on cutoff values in the complete case analysis of the training set

Groups	Sensitivity	Specificity	Upgrade rates	
			Low-risk group	High-risk group
Training set				
0.63[a]	81.4(70/86)	86.7(52/60)	23.5(16/68)	89.7(70/78)
0.18[a]	95.3(82/86)	56.7(34/60)	10.5(4/38)	75.9(82/108)
0.11[a]	98.8(85/86)	38.3(23/60)	4.1(1/24)	69.7(85/122)
Internal validation set				
0.63[a]	77.8(21/27)	90.0(18/20)	25.0(6/24)	91.3(21/23)
0.18[a]	100(27/27)	50.0(10/20)	0	73.0(27/37)
0.11[a]	100(27/27)	35.0(7/20)	0	67.5(27/40)
External validation set				
0.63[a]	73.1(19/26)	90.3(28/31)	20.0(7/35)	86.4(19/22)
0.18[a]	100(26/26)	67.7(21/31)	0	72.2(26/36)
0.11[a]	100(26/26)	41.9(13/31)	0	59.1(26/44)

Note: variables are expressed as numbers of lesions with percentages in parentheses

[a] Cutoff values obtained from the training set

Table 5 Multivariable logistic regression analysis to identify the factors associated with upgrade of atypical ductal hyperplasia with intraductal papilloma at biopsy

Variable	Multivariable Analysis	
	Odds Ratio (95%CI)	*P* Value
Median age (year)	1.06(1.02,1.10)	0.005
Median size (cm)	1.69(0.80,3.58)	0.17
Lesion types		
Mass-like lesion	1 (reference)	
Non-mass-like lesion	2.88(0.58,14.25)	0.19
Margin		
Circumscribed	1 (reference)	
Not circumscribed	1.66(0.54,5.14)	0.38
Calcifications on ultrasound		
Absent	1 (reference)	
Present	2.01(0.34,11.80)	0.44
Ki-67 status		
Negative	1 (reference)	
Positive	3.75(0.79,17.79)	0.10
Unknown	0.20(0.03,1.35)	0.10
Imaging-pathology correlation		
Concordant	1 (reference)	
Discordant	3.67(1.05,12.83)	0.04

Discussion

Accurately predicting ADH lesions that are likely to upgrade to malignant presents a major challenge in individualized risk management. The data of this study showed that the established and validated prediction model incorporating clinical, pathological, and US findings can effectively identify the lesions diagnosed as ADH by CNB but upgraded to malignancy at surgery. The upgrade rate of ADH with intraductal papilloma was 53.8%, and age and imaging-pathological discordance were positively associated with malignancy upgrade.

The independent predictive factors selected from the multivariable analysis were age, the pathological pattern of ADH with intraductal papilloma or ADH alone, Ki-67 positivity, and imaging-pathological discordance. Previous studies have reported the upgrade rates and the risk factors for upgrade in following open excision [11, 12, 19–21]. The target area of the biopsy may be different due to different imaging guidance methods, resulting in different upgrade rates and risk factors. A systematic review and meta-analysis of 6458 lesions showed that the

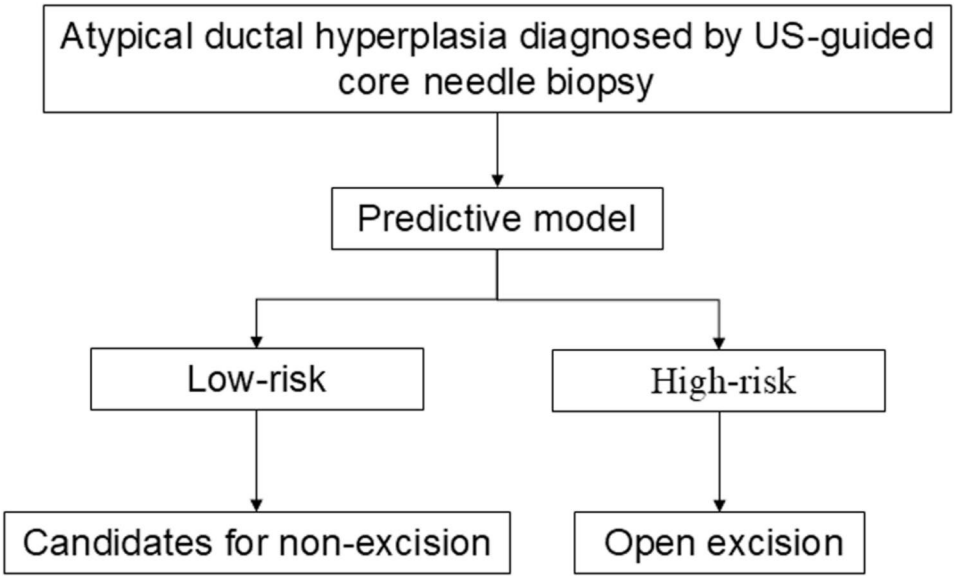

Fig. 7 Flowchart of clinical decision-making

Table 6 Multivariable logistic regression analysis to identify the factors associated with upgrade of atypical ductal hyperplasia alone

Variable	Multivariable Analysis	
	Odds Ratio (95%CI)	*P* Value
Median age (year)	1.18(1.06,1.32)	0.002
Median size (cm)	4.36(4.36,19.78)	0.06
Lesion types		
Mass-like lesion	1 (reference)	
Non-mass-like lesion	0.27(0.01,5.21)	0.38
Shape		
Round/Oval	1 (reference)	
Irregular	3.49(0.11,107.18)	0.47
Margin		
Circumscribed	1 (reference)	
Not circumscribed	1.62(0.19,13.95)	0.66
Calcifications on ultrasound		
Absent	1 (reference)	
Present	1.50(0.13,17.65)	0.78
Vascularity		
Absent	1 (reference)	
Present	1.01(0.17,5.76)	0.99
ER status		
Negative	1 (reference)	
Positive	1.31(0.17,9.96)	0.79
Unknown	2.32(0.04,104.62)	0.69
Ki-67 status		
Negative	1 (reference)	
Positive	79.76(3.85,787.81)	0.005
Unknown	0.66(0.65,6.71)	0.73
Imaging-pathology correlation		
Concordant	1 (reference)	
Discordant	18.87(2.22,160.37)	0.007

Note: ER = estrogen receptor

upgrade rate was 42% for US guidance, 23% for stereotactic biopsy, and 32% for MRI guidance [8]. Models that incorporate different biopsy devices and different image guidance methods may not be reliable for evaluating ADH lesions diagnosed by US-guided CNB. The increasing patient age was previously associated with upgrades, and this finding is in line with our study [12, 22, 23]. Previous studies showed that the imaging-pathology correlation was not useful for predicting upgrades, which was slightly different from our results [11, 12, 20]. The difference may be attributed to the definition of imaging-pathology correlation. As per the Third International Consensus Conference on lesions of uncertain malignant potential in the breast (B3 lesions), general surveillance is not recommended when the upgrade rate of B3 lesions exceeds the defined acceptable limits (10% for DCIS and 5% for invasive carcinoma) [7]. As stated in the ACR BI-RADS®Atlas [16], the likelihood of malignancy is between 2% and 10% for category 4 A, and between 10% and 50% for category 4B. Therefore, for lesions diagnosed with ADH by CNB, it would be more appropriate to categorize lesions as imaging-pathological concordance for categories 3 and 4 A, and imaging-pathological discordance for categories 4B – 5. In addition, for the management of imaging-pathologic discordance, US-guided vacuum-assisted breast biopsy could identify almost 50% of cancers missed by CNB, avoiding surgical biopsies [24]. Compared with CNB, vacuum-assisted biopsy can remove the lesion almost completely, which significantly increases the sample size to reduce sampling error [25]. However, even if the complete resection of the visible lesions on imaging at the time of sampling by vacuum-assisted biopsy, it was still difficult to avoid pathological underestimation, with up to 14% of the lesions being upgraded to malignant post-surgery [8].

The pathological pattern is an important parameter to evaluate the upgrade of ADH lesions. The upgrade rate was lower in ADH lesions co-diagnosed with fibroadenoma or adenosis, but higher in those co-diagnosed with intraductal papilloma and ADH alone. Previous studies have shown that, when co-diagnosed with intraductal papilloma, ADH is associated with progression to malignancy at a rate of 41.7–52.4% [21, 26]. This study found an upgrade rate of 53.8%. Multivariable analysis of ADH co-diagnosed with intraductal papilloma indicated that age and imaging-pathological discordance were independent predictors for upgrade. It is recommended that all older or imaging-pathological discordance patients who diagnosed as ADH with intraductal papilloma undergo surgery. However, this recommendation requires validation with more data in the future.

In this study, the cutting needles utilised exhibited a size range of 18-gauge to 14-gauge, with the size designated by the operator of the biopsy procedure. The selection of the optimum needle size for US-guided CNB of breast lesions remains a matter of some contention. Huang et al. [27]compared the diagnostic accuracy of US-guided CNB of breast masses by different size of cutting needles and found that there was no significant difference in rates of specimen inadequacy, surgical discordance, imaging discordance, DCIS upgrade and high-risk lesion upgrade between 14-gauge, 16-gauge and 18-gauge needles. The study by Giuliani et al. [28]similarly confirmed that US-CNB with small needles, 16 and 18 gauge, had equivalent diagnostic accuracy to that with 14-gauge needles, regardless of breast lesion characteristics. These results are consistent with the data presented in this study. However, several studies have indicated that the employment of a 14-gauge needle in conjunction with ultrasound guidance for breast CNB is to be preferred to the use of a 16-gauge needle [29, 30]. In addition to the size of the cutting needle, the minimum number of samples has varied among previous studies. Fishman et al. [31] proposed that a minimum of four specimens were

required for 14-gauge US-guided breast biopsies. Data from the study by Kirshenbaum et al. showed that the use of 14-gauge CNB in the same breast mass for three sampling yielded a diagnostic yield of 98% [32]. According to the Guidelines for non-operative diagnostic procedures and reporting in breast cancer screening, two or three passes are usually sufficient in most cases to obtain diagnostic material from breast lesions [33]. For US-guided CNB of breast lesions, the quality of the specimens is more important than the number of specimens. Representative specimens can increase the confidence of the pathologist in making a correct diagnosis. Fragmented specimens can make it difficult to provide a definitive diagnosis.

Management strategies must be defined based on the population-level risks and patient perspectives on the associated benefits and risks of interventions. General surveillance is not recommended for B3 lesions with an upgrade rate greater than 10% [13]. This study showed that 51.0% of ADH lesions at CNB were upgraded to malignant at surgery, which exceeds the acceptable limits. It is essential to identify whether ADH lesions are malignant before making treatment decisions or discussing the condition with the patients. The model developed in this study for predicting the upgrade of ADH yielded an AUC of 0.912 in the multiple imputed data sets, 0.915 in the complete case analysis of the training set, 0.906 in the internal validation set, and 0.934 in the external validation set. At a cutoff value of 0.11, the upgrade rate in the training set was 4.1%, indicating that low-risk patients may benefit from non-open excision. Surveillance or risk reduction strategies, rather than open excision, might be appropriate for low-risk patients. The decision curve analysis also showed a positive net benefit when the threshold probability was between 0 and 0.7. Hence, our study provides a reliable supplementary tool for selecting management strategies for ADH lesions diagnosed by CNB.

There are some limitations in our study. Firstly, the model was developed and validated using only retrospective data from two centers. There was a lack of prospective validation with data from more institutions. Secondly, some potentially valuable data, like HER2, were not tested in the model due to the presence of many missing values. Thirdly, this model is only applicable to patients who underwent US examination and US-guided CNB. Applying this model directly to vacuum-assisted biopsy or other imaging guidance methods like stereotactic biopsy and MRI guidance might not generate satisfactory results.

Conclusions

The model established to predict ADH upgrading can help in individualized risk management. If predictors of non-upgraded ADH lesions can be confirmed with larger studies, more than one-third of non-malignant lesions are expected to be candidates for non-excision.

Abbreviations

ADH	atypical ductal hyperplasia
DCIS	ductal carcinoma in situ
CNB	core needle biopsy
AUC	area under the receiver operating characteristic curve
OR	odds ratio
ER	estrogen receptor
PR	progesterone receptor
HER2	human epidermal growth factor receptor 2

Supplementary Information

The online version contains supplementary material available at https://doi.org/10.1186/s12880-025-01707-z.

Supplementary Material 1

Acknowledgements

Not applicable.

Author contributions

All authors contributed to the study conception and design. Material preparation, data collection and analysis were performed by Jun Kang Li, Yong Jie Xu, and Yu Chen Liu. The first draft of the manuscript was written by Jun Kang Li and Yong Jie Xu and all authors commented on previous versions of the manuscript. All authors read and approved the final manuscript.

Funding

This work was supported by the National Key Research and Development Program of China (No. 2023YFC2414203); the National Natural Science Foundation of China (No. 82071925); and the National Natural Science Foundation of China (No. 82371972).

Data availability

Data is provided within the manuscript or supplementary information files.

Declarations

Ethics approval and consent to participate

This retrospective study was approved by the Medical Ethics Committee of Chinese PLA General Hospital (No. S2021-683-01). Informed consent was waived because of the retrospective design. The study was performed in accordance with the Declaration of Helsinki.

Consent for publication

All authors gave their approval for manuscript's publication. As a retrospective study, patient informed consent (e.g., reproduced images) was waived.

Competing interests

The authors declare no competing interests.

Author details

[1]Department of Ultrasound, The First Medical Center, Chinese PLA General Hospital, Beijing, China
[2]Department of Ultrasound, Chinese PLA 63820 Hospital, Mianyang, Sichuan, China
[3]Department of Ultrasound Diagnosis, The Ninth Medical Center, Chinese PLA General Hospital, Beijing, China
[4]Department of Gastroenterology, Chinese PLA 63820 Hospital, Mianyang, Sichuan, China

[5]The First Medical Center, Chinese PLA General Hospital, 28 Fuxing Road, Beijing 100853, China

Received: 9 December 2024 / Accepted: 5 May 2025
Published online: 19 May 2025

References

1. Lakhani S, Ellis I, Schnitt S, Tan P, Mj VDV. World health organization classification of tumours of the breast. Lyon: International Agency for Research on Cancer; 2012.
2. Morrow M, Schnitt SJ, Norton L. Current management of lesions associated with an increased risk of breast cancer. Nat Rev Clin Oncol. 2015;12(4):227–38.
3. Lewin AA, Mercado CL. Atypical ductal hyperplasia and lobular neoplasia: update and easing of guidelines. AJR Am J Roentgenol. 2020;214(2):265–75.
4. Burbank F. Stereotactic breast biopsy of atypical ductal hyperplasia and ductal carcinoma in situ lesions: improved accuracy with directional, vacuum-assisted biopsy. Radiology. 1997;202(3):843–7.
5. Wei X, Li Y, Zhang S, Zhu Y, Fan Y. Experience in large-core needle biopsy in the diagnosis of 1431 breast lesions. Med Oncol. 2011;28(2):429–33.
6. Bulletins ACoOaGCoP. Practice bulletin 164: diagnosis and management of benign breast disorders. Obstet Gynecol. 2016;127(6):e141–56.
7. Elfgen C, Leo C, Kubik-Huch RA, Muenst S, Schmidt N, Quinn C, McNally S, van Diest PJ, Mann RM, Bago-Horvath Z, et al. Third international consensus conference on lesions of uncertain malignant potential in the breast (B3 lesions). Virchows Arch. 2023;483(1):5–20.
8. Schiaffino S, Calabrese M, Melani EF, Trimboli RM, Cozzi A, Carbonaro LA, Di Leo G, Sardanelli F. Upgrade rate of percutaneously diagnosed pure atypical ductal hyperplasia: systematic review and Meta-Analysis of 6458 lesions. Radiology. 2020;294(1):76–86.
9. Bicchierai G, Pugliese F, Amato F, De Benedetto D, Boeri C, Vanzi E, Di Naro F, Bianchi S, Cossu E, Miele V, et al. Percutaneous vacuum-assisted excision (VAE) of breast lesions of uncertain malignant potential (B3 lesions): a preliminary single-centre Italian experience. Radiol Med. 2023;128(5):528–36.
10. Chen LY, Hu J, Tsang JYS, Lee MA, Ni YB, Chan SK, Tse GMK. Diagnostic upgrade of atypical ductal hyperplasia of the breast based on evaluation of histopathological features and calcification on core needle biopsy. Histopathology. 2019;75(3):320–8.
11. Huang YX, Chen YL, Li SP, Shen JP, Zuo K, Zhou SC, Chang C. Development and validation of a Simple-to-Use nomogram for predicting the upgrade of atypical ductal hyperplasia on core needle biopsy in Ultrasound-Detected breast lesions. Front Oncol. 2020;10:609841.
12. Ko E, Han W, Lee JW, Cho J, Kim EK, Jung SY, Kang MJ, Moon WK, Park IA, Kim SW, et al. Scoring system for predicting malignancy in patients diagnosed with atypical ductal hyperplasia at ultrasound-guided core needle biopsy. Breast Cancer Res Treat. 2008;112(1):189–95.
13. Rageth CJ, O'Flynn EAM, Pinker K, Kubik-Huch RA, Mundinger A, Decker T, Tausch C, Dammann F, Baltzer PA, Fallenberg EM et al. Second International Consensus Conference on lesions of uncertain malignant potential in the breast (B3 lesions). Breast Cancer Res. Treat. 2019;174(2):279–96.
14. Goldhirsch A, Wood WC, Coates AS, Gelber RD, Thurlimann B, Senn HJ. Panel m: strategies for subtypes–dealing with the diversity of breast cancer: highlights of the St. Gallen international expert consensus on the primary therapy of early breast Cancer 2011. Ann Oncol. 2011;22(8):1736–47.
15. Li JK, Wang HF, He Y, Huang Y, Liu G, Wang ZL. Ultrasonographic features of ductal carcinoma in situ: analysis of 219 lesions. Gland Surg. 2020;9(6):1945–54.
16. Mendelson EB, Böhm-Vélez M, Berg WA, Whitman GJ, Feldman MI, Madjar H, Rizzatto G, Baker JA. ACR BI-RADS ultrasound. In: ACR BI-RADS Atlas, breast imaging reporting and data system, 5th edition. Reston, Va: American College of Radiology; 2013.
17. MedCalc Software Ltd. Odds ratio calculator. https://www.medcalc.org/calc/odds_ratio.php, 2023 (Accessed July 17 2024).
18. van Buuren S. Multiple imputation of discrete and continuous data by fully conditional specification. Stat Methods Med Res. 2007;16(3):219–42.
19. Pena A, Shah SS, Fazzio RT, Hoskin TL, Brahmbhatt RD, Hieken TJ, Jakub JW, Boughey JC, Visscher DW, Degnim AC. Multivariate model to identify women at low risk of cancer upgrade after a core needle biopsy diagnosis of atypical ductal hyperplasia. Breast Cancer Res Treat. 2017;164(2):295–304.
20. Mesurolle B, Perez JC, Azzumea F, Lemercier E, Xie X, Aldis A, Omeroglu A, Meterissian S. Atypical ductal hyperplasia diagnosed at sonographically guided core needle biopsy: frequency, final surgical outcome, and factors associated with underestimation. AJR Am J Roentgenol. 2014;202(6):1389–94.
21. Deshaies I, Provencher L, Jacob S, Cote G, Robert J, Desbiens C, Poirier B, Hogue JC, Vachon E, Diorio C. Factors associated with upgrading to malignancy at surgery of atypical ductal hyperplasia diagnosed on core biopsy. Breast. 2011;20(1):50–5.
22. Sutton T, Farinola M, Johnson N, Garreau JR. Atypical ductal hyperplasia: clinicopathologic factors are not predictive of upgrade after excisional biopsy. Am J Surg. 2019;217(5):848–50.
23. Chae BJ, Lee A, Song BJ, Jung SS. Predictive factors for breast cancer in patients diagnosed atypical ductal hyperplasia at core needle biopsy. World J Surg Oncol. 2009;7:77.
24. Vatteroni G, Pinna G, Trimboli RM, Levi R, Bolengo I, Patrone F, Volpe D, Fernandes B, Bernardi D. Role of ultrasound-guided vacuum-assisted breast biopsy in the management of radiologic-pathologic discordance: a retrospective single-centre study. Radiol Med. 2024;129(10):1454–62.
25. Wang ZL, Liu G, Li JL, Su L, Liu XJ, Wang W, Tang J. Breast lesions with imaging-histologic discordance during 16-gauge core needle biopsy system: would vacuum-assisted removal get significantly more definitive histologic diagnosis than vacuum-assisted biopsy? Breast J. 2011;17(5):456–61.
26. Karwowski P, Lumley D, Stokes D, Pavlica M, Edsall B, Fu S, Francfort J, Cohen B, Capizzi A, Ma ZW, et al. Atypical ductal hyperplasia on core needle biopsy: surgical outcomes of 200 consecutive cases from a high-volume breast program. Breast J. 2021;27(3):287–90.
27. Huang ML, Hess K, Candelaria RP, Eghtedari M, Adrada BE, Sneige N, Fornage BD. Comparison of the accuracy of US-guided biopsy of breast masses performed with 14-gauge, 16-gauge and 18-gauge automated cutting needle biopsy devices, and review of the literature. Eur Radiol. 2017;27(7):2928–33.
28. Giuliani M, Rinaldi P, Rella R, Fabrizi G, Petta F, Carlino G, Di Leone A, Mule A, Bufi E, Romani M, et al. Effect of needle size in Ultrasound-guided core needle breast biopsy: comparison of 14-, 16-, and 18-Gauge needles. Clin Breast Cancer. 2017;17(7):536–43.
29. Lai HW, Wu HK, Kuo SJ, Chen ST, Tseng HS, Tseng LM, Chen DR. Differences in accuracy and underestimation rates for 14- versus 16-gauge core needle biopsies in ultrasound-detectable breast lesions. Asian J Surg. 2013;36(2):83–8.
30. Gruber I, Oberlechner E, Heck K, Hoopmann U, Boer B, Fugunt R, Gall C, Hartkopf AD, Helms G, Hoffmann SM, et al. Percutaneous Ultrasound-Guided core needle biopsy: comparison of 16-Gauge versus 14-Gauge needle and the effect of coaxial guidance in 1065 breast Biopsies - A prospective randomized clinical noninferiority trial. Ultraschall Med. 2020;41(5):534–43.
31. Fishman JE, Milikowski C, Ramsinghani R, Velasquez MV, Aviram G. US-guided core-needle biopsy of the breast: how many specimens are necessary? Radiology. 2003;226(3):779–82.
32. Kirshenbaum K, Keppke A, Hou K, Dickerson M, Gajjar M, Kirshenbaum G. Reassessing specimen number and diagnostic yield of ultrasound guided breast core biopsy. Breast J. 2012;18(5):464–9.
33. Lee AH, Carder R, et al. Guidelines for non-operative diagnostic procedures and reporting in breast cancer screening. London, UK: Royal College of Pathologists; 2021.

Publisher's note